Journal of Applied Fluid Mechanics, Vol. 9, No. 2, pp. 519-527, 2016.
Available online at www.jafmonline.net, ISSN 1735-3572, EISSN 1735-3645.
DOI: 10.18869/acadpub.jafm.68.225.24433

Onset of Convection in a Nanofluid Layer Confined within a Hele-Shaw Cell

D. Yadav and J. Lee†

School of Mechanical Engineering, Yonsei University, Seoul 120 749, South Korea

†*Corresponding Author Email: jinholee@yonsei.ac.kr*

(Received December 29, 2014; accepted February 6, 2015)

ABSTRACT

In this study, the onset of nanofluid convection confined within a Hele-Shaw cell is investigated by performing a classical linear stability analysis. The model used for nanofluid combines the effects of Brownian motion and thermophoresis, while for Hele-Shaw cell Brinkman model are employed. The new stability equations are formulated by introducing new characteristic dimensionless parameters such as the Hele-Shaw number, the Hele-Shaw Rayleigh number and the nanoparticle concentration Hele-Shaw Rayleigh number. The resulting stability equations are solved numerically by using higher order Galerkin method. It is found that the nanoparticle concentration Hele-Shaw Rayleigh number, the Lewis number and the modified diffusivity ratio hasten the onset of convection, while the Hele-Shaw number delays the onset of convection. A comparison is also made between the existing boundary conditions for nanoparticle and obtained that the zero nanoparticle flux boundary conditions under the thermophoretic effects has more destabilizing effect than the fixed nanoparticle boundary conditions.

KEYWORDS: Nanofluid convection; Brownian motion; Thermophoresis; Hele-Shaw cell.

1. INTRODUCTION

This paper concerns the stability of a nanofluid layer confined within a Hele-Shaw cell, heated from below. A Hele-Shaw cell is a device, whose essential features are two parallel flat plates separated by an infinitesimally small gap containing a thin layer of fluid. Various problems in fluid mechanics can be approximated to Hele-Shaw flows and thus the study of these flows is of significance. Nowadays, the Hele-Shaw flow is used in several fields of natural sciences and engineering, in particular, matter physics, materials science and crystal growth due to manufacturing techniques. The equations governing the flow of the fluid in the Hele-Shaw cell are similar to those governing the flow in a saturated porous medium. Hele–Shaw (1898) was the first who showed the analogy between the two-dimensional flow in a porous medium and Hele-Shaw cell by defining an equivalent permeability of $b^2/12$ for the Hele-Shaw cell where b is the width of the fluid layer gap. Several authors have attempted to find the limits of applicability for this analogy. Wooding (1961), Elder (1967), Hartline and Lister (1977), Kvernvold (1979) and Bhadauria *et al*. (2005) used free convection in Hele–Shaw cells to simulate thermal convection in porous media. By properly identifying the Hele-Shaw permeability, they have demonstrated that the Hele-Shaw cell can be a powerful tool for quantitative study of two-dimensional flow in porous media.

Recently, there has been significant interest in nanofluids due to need of heat transfer enhancement. The term 'nanofluid' denotes a mixture of solid nanoparticles and a common base fluid. Nanoparticles used in nanofluid have diameters below 100 nm. Due to their small size, nanoparticles dissolved easily inside the base fluid, and as a result, jam of channels and erosion in channel walls do not happen. In occurrence of a simple few percents of nanoparticles, a significant increase of the effective thermal conductivity of nanofluids has been found (Xuan and Li 2000; Das *et al*. 2006; Aybar *et al*. 2014; Malvandi 2015). The properties of nanofluids have made them potentially useful in many practical applications in industrial, commercial, residential and transportation sectors (Manna 2009; Yu and Xie 2012).

Buongiorno (2006) developed a model for nanofluid incorporating the effects of Brownian diffusion and thermophoresis. Using that model, Tzou (2008), Nield and Kuznetsov (2009, 2011a, 2011b), Kuznetsov and Nield (2010a,b,c), Rana *et al*. (2014), Chand *et al*. (2012a,b, 2015), Hayat *et al*. (2015), Umavathi and Mohite (2014), Yadav *et al*. (2011, 2012a,b, 2013a,b,c, 2014a,b) and Bhadauria and Agrawal (2011a,b,c) studied the

problem related to thermal instability in nanofluids. In all of those studies, the nanoparticle volumetric fraction on the boundaries was fixed which is quite hard to recognize physically. Very recently, Nield and Kuznetsov (2014) and Agrawal (2014) studied thermal instability in a porous medium layer saturated by a nanofluid using the Darcy model with a very new set of boundary condition that the nanoparticle flux is assumed to be zero rather than prescribing the nanoparticle volumetric fraction on the boundaries. This shows that nanoparticle fraction value at the boundary adjusts accordingly.

The objective of the present investigation is to study the onset of convection in a nanofluid layer confined within a Hele-Shaw cell using the Brinkman's model with the new set of boundary conditions. The new stability equations are derived which are solved numerically by using higher order Galerkin method. The effects of the Hele-Shaw number and the nanoparticle parameters on the onset of convection are studied. To the best of authors' knowledge this type of investigation is still to be added in the literature of the nanofluid flow.

2. PROBLEM FORMULATIONS

Consider a nanofluid layer of height d, vertically confined between two parallel rigid impermeable boundaries at $z^* = 0$ and $z^* = d$, which are maintained at constant but different temperature T_h^* and T_c^* ($T_h^* > T_c^*$), respectively. The nanofluid shall be infinitely extended in the x-direction, but confined in the y-direction by vertical impermeable boundaries (sidewalls) at $y^* = 0$ and $y^* = b$ ($\ll d$). The schematic diagram of the system considered here is as shown in Fig.1. Asterisks are used to distinguish the dimensional variables from the non-dimensional variables (without asterisks).

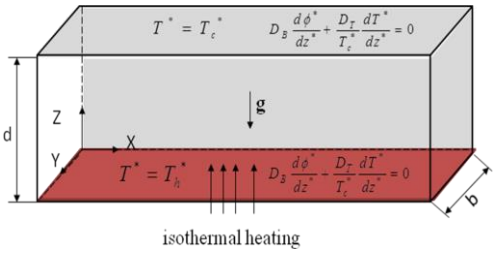

Fig. 1. Physical configuration of the system considered.

2.1 Assumptions

The mathematical equations describing the physical model are based upon the following assumptions:

(i) Nanofluid is dilute and nanoparticles are suspended in the nanofluid using either surfactant or surface charge technology. This shows that the stratified state has had no time to be settled and nanofluid behaves like pure fluid.

(ii) The thermophysical properties except for density in the buoyancy force (Boussinesq hypothesis) are constant for the purpose of characterization and estimates of the various effects on the order of magnitude.

(iii) The fluid phase and nanoparticles are in thermal equilibrium state.

(iv) Nanoparticles are spherical.

(v) Nanofluid is incompressible, Newtonian and laminar;

(vi) Each boundary wall is assumed to be impermeable and perfectly thermal conducting.

(vii) Radiative heat transfer between the sides of wall is negligible when compared with other modes of the heat transfer.

2.2 Governing Equations

When the Hele-Shaw cell gap width is not sufficiently small with regard to the appearing wavelength of the instability, the correction to Darcy's law is needed. Therefore, on employing the Brinkman model, the governing equations formulated by Buongiorno (2006) and Nield and Kuznetsov (2009) with Hele-Shaw approximation are:

$$\nabla^* \cdot \vec{\mathbf{v}}^* = 0, \tag{1}$$

$$\rho_c \left[\frac{\partial}{\partial t^*} + \left(\vec{\mathbf{v}}^* \cdot \nabla^*\right)\right]\vec{\mathbf{v}}^* = -\nabla^* p^* - \frac{\mu}{K}\vec{\mathbf{v}}^* + \mu\nabla^{*2}\vec{\mathbf{v}}^* + \left[\phi^*\rho_p + \rho_c\left(1-\phi^*\right) \times\left\{1-\beta\left(T^* - T_c^*\right)\right\}\right]\vec{\mathbf{g}}, \tag{2}$$

$$\left[\frac{\partial}{\partial t^*} + \left(\mathbf{v}^* \cdot \nabla^*\right)\right]T^* = \alpha\nabla^{*2}T^* + \frac{(\rho c)_p}{(\rho c)} \times\left[D_B\nabla^*\phi^* \cdot \nabla^* T^* + \left(\frac{D_T}{T_c^*}\right)\nabla^* T^* \cdot \nabla^* T^*\right], \tag{3}$$

$$\left[\frac{\partial}{\partial t^*} + \left(\vec{\mathbf{v}}^* . \nabla^*\right)\right]\phi^* = D_B\nabla^{*2}\phi^* + \frac{D_T}{T_c^*}\nabla^{*2}T^*, \tag{4}$$

with the boundary conditions as:

$$w^* = \frac{dw^*}{dz^*} = 0,\ T^* = T_h^*,\quad D_B\frac{d\phi^*}{dz^*} + \frac{D_T}{T_c^*}\frac{dT^*}{dz^*} = 0, \quad \text{at} \quad z^* = 0, \tag{5a}$$

$$w^* = \frac{dw^*}{dz^*} = 0,\ T^* = T_c^*,\quad D_B\frac{d\phi^*}{dz^*} + \frac{D_T}{T_c^*}\frac{dT^*}{dz^*} = 0 \quad \text{at} \quad z^* = d. \tag{5b}$$

In these equations, subscripts p and c refer to the nanoparticles and a reference quantity, respectively, $\vec{\mathbf{v}}^* = \left(u^*, v^*, w^*\right)$ is the nanofluid velocity, $K = b^2/12$ is the permeability of the fluid flow, ϕ^* is the nanoparticle volumetric fraction, T^* is the temperature, D_B is the Brownian diffusion coefficient, D_T is the thermophoresis diffusion coefficient, $\vec{\mathbf{g}}$ is the gravitational acceleration, (ρc) is the heat capacity, β_T is the thermal volumetric expansion coefficient, μ is the viscosity, ρ is density and k is the thermal conductivity of the nanofluid.

To write the governing equations in the non-dimensional form, we introduce the following scales:

$$(x, y, z) = \frac{\left(x^*, y^*, z^*\right)}{d},\ \tau = \frac{t^*\alpha}{d^2},\ \vec{\mathbf{v}} = \frac{\vec{\mathbf{v}}^* d}{\alpha},$$
$$p = \frac{p^* d^2}{\mu\alpha},\ \phi = \frac{\phi^* - \phi_c^*}{\phi_c^*},\ \theta = \frac{T^* - T_c^*}{T_h^* - T_c^*}. \quad (6)$$

The non-dimensional form of equations (1)-(5) with the help of equations (6) become as:

$$\nabla \cdot \vec{\mathbf{v}} = 0, \quad (7)$$

$$\frac{H_S}{P_r}\left[\frac{\partial}{\partial\tau} + \left(\vec{\mathbf{v}}\cdot\nabla\right)\right]\vec{\mathbf{v}} = -\nabla\tilde{p} + H_S\nabla^2\vec{\mathbf{v}} - \vec{\mathbf{v}} + R_H\theta\hat{e}_z - R_{nH}\phi\hat{e}_z, \quad (8)$$

$$\left[\frac{\partial}{\partial\tau} + \left(\vec{\mathbf{v}}\cdot\nabla\right)\right]\theta = \nabla^2\theta + \frac{N_B}{L_e}\nabla\phi\cdot\nabla\theta + \frac{N_A N_B}{L_e}\nabla\theta\cdot\nabla\theta, \quad (9)$$

$$\left[\frac{\partial}{\partial\tau} + \left(\vec{\mathbf{v}}\cdot\nabla\right)\right]\phi = \frac{1}{L_e}\nabla^2\phi + \frac{N_A}{L_e}\nabla^2\theta, \quad (10)$$

with boundary conditions as:

$$w = \frac{dw}{dz} = 0,\ \theta = 1,\ \frac{d\phi}{dz} + N_A\frac{d\theta}{dz} = 0 \quad \text{at } z = 0 \quad (11a)$$

$$w = \frac{dw}{dz} = 0,\ \theta = 0,\ \frac{d\phi}{dz} + N_A\frac{d\theta}{dz} = 0 \quad \text{at } z = 1. \quad (11b)$$

Here $\nabla\tilde{p} = \nabla p + R_{mH}\hat{e}_z$. The non-dimensional parameters that appear in the equations (7)-(11) are defined as:

$R_H = \frac{\rho_c g \beta_T K d (T_h^* - T_c^*)}{\mu\alpha}$ is the Hele-Shaw Rayleigh number, $R_{mH} = \frac{\{\rho_p\phi_c^* + \rho_c(1-\phi_c^*)\}gKd}{\mu\alpha}$ is the basic-density Hele-Shaw Rayleigh number, $R_{nH} = \frac{\left(\rho_p - \rho_c\right)\phi_c^* gKd}{\mu\alpha}$ is the nanoparticle concentration Hele-Shaw Rayleigh number, $P_r = \frac{\nu}{\alpha}$ is the Prandtl number, $H_S = \frac{K}{d^2}$ is the Hele-Shaw number, $L_e = \frac{\alpha}{D_B}$ is the Lewis number, $N_A = \frac{D_T\left(T_h^* - T_c^*\right)}{D_B T_c^* \phi_c^*}$ is the modified diffusivity ratio and $N_B = \frac{(\rho c)_p \phi_c^*}{(\rho c)}$ is the modified particle density increment.

3. BASIC SOLUTION

The basic state of the nanofluid is assumed to be time independent and is described by

$$\vec{\mathbf{v}} = 0,\ \theta = \theta_b(z),\ p = p_b(z),\ \phi = \phi_b(z). \quad (12)$$

Then Eqs (9) and (10) become:

$$\frac{d^2\theta_b}{dz^2} + \frac{N_B}{L_e}\frac{d\phi_b}{dz}\frac{d\theta_b}{dz} + \frac{N_A N_B}{L_e}\left(\frac{d\theta_b}{dz}\right)^2 = 0, \quad (13)$$

$$\frac{d^2\phi_b}{dz^2} + N_A\frac{d^2\theta_b}{dz^2} = 0, \quad (14)$$

under the following boundary conditions:

$$\theta_b = 1,\ \frac{d\phi_b}{dz} + N_A\frac{d\theta_b}{dz} = 0 \quad \text{at } z = 0, \quad (15a)$$

$$\theta_b = 0,\ \frac{d\phi_b}{dz} + N_A\frac{d\theta_b}{dz} = 0 \quad \text{at } z = 1. \quad (15b)$$

On solving equations (13) and (14) subject to the above boundary conditions (15), we have

$$\theta_b = 1 - z \text{ and } \phi_b = \phi_c^* + N_A z, \quad (16a,b)$$

where ϕ_c^* is the reference value of nanoparticle volume fraction.

4. PERTURBATION EQUATIONS

For small disturbances onto the primary flow, we assume that:

$$\vec{\mathbf{v}} = \vec{\mathbf{v}}',\ \rho = \rho_b(z) + \rho',\ \tilde{p} = p_b(z) + p',$$
$$\theta = \theta_b(z) + \theta',\ \phi = \phi_b(z) + \phi', \quad (17)$$

where prime indicates perturbation quantities over their equilibrium counterparts and assumed to be small. On substituting equation (17) into equations (7) - (11) and neglecting the product of prime quantities, we have:

$$\nabla \cdot \vec{\mathbf{v}}' = 0, \tag{18}$$

$$\frac{H_S}{P_r}\frac{\partial \vec{\mathbf{v}}'}{\partial \tau} = -\nabla p' + H_S \nabla^2 \vec{\mathbf{v}}' - \vec{\mathbf{v}}' + R_H \theta' \hat{e}_z - R_{nH} \phi' \hat{e}_z , \tag{19}$$

$$\frac{\partial \theta'}{\partial \tau} - w' = \nabla^2 \theta' - \frac{N_B}{L_e}\left(N_A \frac{\partial \theta'}{\partial z} + \frac{\partial \phi'}{\partial z} \right), \tag{20}$$

$$\frac{\partial \phi'}{\partial \tau} + N_A w' = \frac{1}{L_e}\nabla^2 \phi' + \frac{N_A}{L_e}\nabla^2 \theta', \tag{21}$$

Operating on Eq. (19) with $\hat{\mathbf{e}}_\mathbf{z} \cdot \nabla \times \nabla \times$ and using the identity $\nabla \times \nabla \times = \nabla\, \nabla \cdot - \nabla^2$ together with Eq. (18), we obtain z -component of the momentum equation as:

$$\left[H_S \nabla^2 - 1 - \frac{H_S}{P_r}\frac{\partial}{\partial \tau} \right] \nabla^2 w' + R_H \nabla_p{}^2 \theta' - R_{nH} \nabla_P{}^2 \phi' = 0, \tag{22}$$

where $\nabla_P{}^2$ is the Laplacian operator in the horizontal plane.

Very recently, Nield and Kuznetsov (2014) observed that the oscillatory convection cannot occur with this new set of boundary conditions due to absence of the two opposing agencies who affect the instability. Therefore, in the absence of oscillatory convection, we can take the perturbation quantities are of the form:

$$\left(w',\ \theta',\ \phi' \right) = \left[W(z),\ \Theta(z),\ \Phi(z) \right] \times \exp\left[ik_x x + ik_y y \right], \tag{23}$$

where k_x, k_y are the wave number along the x and y directions respectively and $a = \sqrt{k_x{}^2 + k_y{}^2}$ is the resultant wave number.

On substituting equation (23) into the differential equations (20), (21) and (22), the linearized equations in dimensionless form are as follows:

$$W + \left(D^2 - \frac{N_A N_B}{L_e} D - a^2 \right)\Theta - \frac{N_B}{L_e} D\Phi = 0, \tag{24}$$

$$-N_A W + \frac{N_A}{L_e}\left(D^2 - a^2 \right)\Theta + \frac{1}{L_e}\left(D^2 - a^2 \right)\Phi = 0, \tag{25}$$

$$\left[H_S \left(D^2 - a^2 \right) - 1 \right]\left(D^2 - a^2 \right) W - R_H a^2 \Theta + R_{nH} a^2 \Phi = 0, \tag{26}$$

and the boundary conditions become:

$$W = DW = \Theta = 0, \quad \mathrm{D}\Phi + N_A D\Theta = 0 \quad \text{at } z = 0 \text{ and } 1, \tag{27}$$

where $D \equiv \frac{d}{dZ}$.

5. METHOD OF SOLUTION

Equations (24)–(26) together with the boundary conditions (27) constitute a linear eigenvalue problem of the system. The resulting eigenvalue problem is solved numerically using the Galerkin weighted residuals method. In this method, the test (weighted) functions are the same as the base (trial) functions. Accordingly W, Θ and Φ are taken in the following way:

$$W = \sum_{s=1}^{N} A_s W_s,\ \Theta = \sum_{s=1}^{N} B_s \Theta_s,\ \Phi = \sum_{s=1}^{N} C_s \Phi_s, \tag{28}$$

where A_s, B_s and C_s are constants. The base functions W_s, Θ_s and Φ_s represented by power series as trivial functions satisfying the respective boundary conditions and are assumed in the following form:

$$W_s = z^{s+1} - 2z^{s+2} + z^{s+3},\ \Theta_s = z^s - z^{s+1},\ \Phi_s = N_A\left(z^{s+1} - z^s \right),\ s = 1,\ 2,\ 3,... \tag{29}$$

Using equation (28) into equations (24)-(26) and multiplying Eq. (24) by Θ_s, Eq. (25) by Φ_s and Eq. (26) by W_s; performing the integration by parts with respect to z between $z = 0$ and 1, we obtain the following system of algebraic equations:

$$\begin{aligned} D_{js} A_s + E_{js} B_s + F_{js} C_s &= 0, \\ G_{js} A_s + H_{js} B_s + I_{js} C_s &= 0, \\ J_{js} A_s + K_{js} B_s + L_{js} C_s &= 0. \end{aligned} \tag{30}$$

The coefficients D_{js} to L_{js} involve inner products of the base functions and are given by:

$$D_{js} = < \Theta_j W_s >,$$

$$E_{js} = < D\Theta_j D\Theta_s - \frac{N_A N_B}{L_e}\Theta_j D\Theta_s - a^2 \Theta_j \Theta_s >,$$

$$F_{js} = < -\frac{N_B}{L_e}\Theta_j D\Phi_s >, \qquad G_{js} = < -N_A \Phi_j W_s >,$$

$$H_{js} = < \frac{N_A}{L_e}\left(D\Phi_j D\Theta_s - a^2 \Phi_j \Theta_s \right) >,$$

$$I_{js} = < \frac{1}{L_e}\left(D\Phi_j D\Phi_s - a^2 \Phi_j \Phi_s \right) >$$

$$J_{js} = < H_S \left(D^2 W_j D^2 W_s - 2a^2 DW_j DW_s + a^4 W_j W_s \right) - \left(DW_j DW_s - a^2 W_j W_s \right) >,$$

$$K_{js} = < -R_H a^2 W_j \Theta_s > \text{ and}$$

$$L_{js} = < R_{nH} a^2 W_j \Phi_s >. \text{ Here } < fg > = \int_0^1 fg\, dz .$$

The above system of homogeneous algebraic equations (30) can have a nontrivial solution if and only if

$$\begin{vmatrix} D_{js} & \mathrm{E}_{js} & \mathrm{F}_{js} \\ G_{js} & \mathrm{H}_{js} & \mathrm{I}_{js} \\ J_{js} & \mathrm{K}_{js} & \mathrm{L}_{js} \end{vmatrix} = 0. \qquad (31)$$

The inner products involved in the determined are evaluated analytically rather than numerically in order to avoid errors in the numerical integration. Equation (31) gives a relation between R_H and a for a fixed value of other parameters. The critical Hele-Shaw Rayleigh number $R_{H,c}$ is obtained by minimizing R_H with respect to the wave number a for different fixed values of the other parameters using the Newton's and golden section search methods. Thus the critical stability parameters $\left(R_{H,c}, a_c\right)$ are computed for different values of physical parameters involved therein. Convergence of the results is achieved by using six terms in the Galerkin expansion.

6. RESULTS AND DISCUSSION

The effect of Hele-Shaw number on the onset of convection in a nanofluid layer is examined by considering a physically more realistic boundary condition on volume fraction of nanoparticles. For the boundary conditions considered, it is not possible to obtain exact analytical solution using single-term Galerkin method, and therefore we have to resort 6-term Galerkin method to solve the resulting eigenvalue problem for different values of the Hele-Shaw number H_S, the nanoparticle concentration Hele-Shaw Rayleigh number R_{nH}, the modified diffusivity ratio N_A, the modified particle density increment N_B and the Lewis number L_e. The Newton-Raphson method is used to obtain the Hele-Shaw Rayleigh number R_H as a function of wave number a and the bisection method is built in to locate the critical stability parameters $(R_{H,c}, a_c)$. The parametric values vary with the base fluid and nanoparticles chosen. According to Buongiorno (2006), Kuznetsov (2011) and Yadav *et al.* (2014c), we have taken the values of nanoparticle concentration Hele-Shaw Rayleigh number R_{nH} in the order $1 \sim 10$, modified particle density increment N_B of the order $10^{-3} \sim 10^{-2}$ and Lewis number is taken in the order of $1 \sim 10^2$. The value of modified diffusivity ratio N_A is not more than 10. The range of these parameters has been predicted using available experimental range of thermo-physical properties of alumina-water nanofluid (Buongiorno 2006; Wong and Kurma 2008).

In order to validate the exactness of the present results, first test computations are carried out in the absence of nanoparticles, i.e. for regular fluid by taking $\phi_c^* = R_{nH} = 0$. The regular critical thermal Rayleigh number R_c and the corresponding critical wave number a_c for different values of Hele-Shaw number H_S are computed for regular fluid. The computed values are tabled in Table 1 and compared with Guo and Kaloni (1995). It is seen that our results are in excellent agreement. These comparisons verify the accuracy of the numerical method used in the present study.

Table 1 $R_{H,c}$ and $a_c{}^2$ for different values of H_s with Guo and Kaloni (1995) for regular fluid

H_s	Guo and Kaloni (1995)		Present study	
	$R_{H,c}$	$a_c{}^2$	$R_{H,c}$	$a_c{}^2$
0.01	60.36	10.47	60.395	10.439
0.1	215.06	9.92	215.02	9.923
1	1752.20	9.70	1751.871	9.734
∞	1707.70	9.71	1707.760	9.709

The significant characteristics of the Hele-Shaw number H_S and the nanoparticle concentration Hele-Shaw Rayleigh number R_{nH} on the stability of the system are exhibited graphically in Figs.2 and 3.

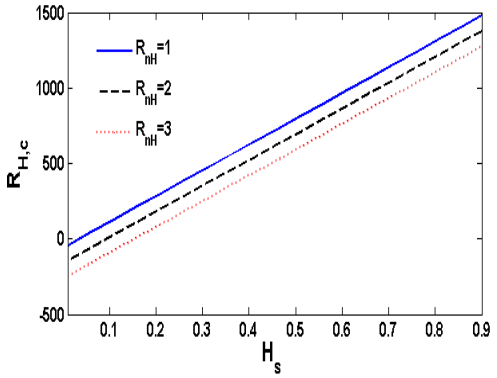

Fig. 2. Effect of the Hele-Shaw number H_s on the critical Hele-Shaw Rayleigh number $R_{H,c}$ for different values of nanoparticle concentration Hele-Shaw Rayleigh number R_{nH} with $N_A = 2$, $\mathrm{N_B} = 0.01$, $L_e = 50$.

From Fig. 2, we see that an increase in the values of H_S is to increase the critical Hele-Shaw Rayleigh number $R_{H,c}$ and hence its effect is to delay the onset of nanofluid convection. This may be quality to the fact that increasing Hele-Shaw number H_S amounts to increase in the permeability of the Hele-Shaw cell i.e. increase in the width of Hele-Shaw cell and hence higher heating is required for the onset of convection.

From Fig. 2, it is also found that the when the nanoparticle concentration Hele-Shaw Rayleigh number R_{nH} increases, in terms of the smaller

value of the critical Hele-Shaw Rayleigh number $R_{H,c}$, the system becomes more unstable. This may be interpreted as an increase in the nanoparticle concentration Hele-Shaw Rayleigh number R_{nH}, increase the Brownian motion and thermophoresis diffusion of the nanoparticles by increasing the volumetric fraction of nanoparticle, which causes destabilizing effect. The corresponding critical wave number a_c is plotted in Fig. 3 and shows that an increase in the values of Hele-Shaw number H_S tends to decrease a_c and thus its effects is to make higher the size of convection cells, while the size of convection cells does not depend on the nanoparticle concentration Hele-Shaw Rayleigh number R_{nH}.

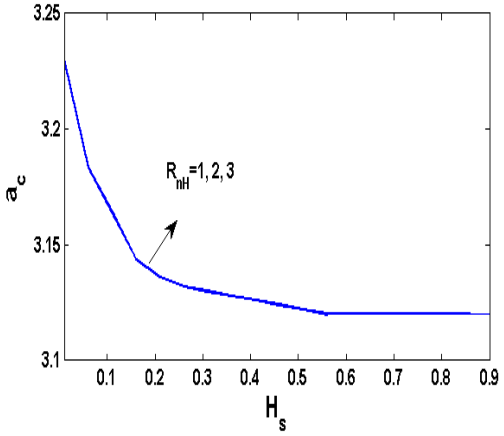

Fig. 3. Effect of the Hele-Shaw number H_s on the critical wave number a_c for different values of nanoparticle concentration Hele-Shaw Rayleigh number R_{nH} with $N_A = 2,\ \mathrm{N_B} = 0.01,\ L_e = 50.$

The effect of modified particle density increment N_B on the onset of convection is made clear in Figs. 4 and 5. From these figures, we observed that the modified particle density increment N_B has no significant effect on the stability of nanofluids convection. This is because the terms containing N_B involves as a function of $\frac{N_B}{L_e}$ and the value of $\frac{N_B}{L_e}$ is too small of order $10^{-2} \sim 10^{-5}$, pointing to the zero contribution of the nanoparticle flux in the thermal energy conversation. The effect of the Hele-Shaw number H_S is same as obtained in Figs. 2 and 3.

To consider the effects of the Lewis number L_e and the modified diffusivity ratio N_A on the stability of the system, the variation of critical Hele-Shaw Rayleigh number $R_{H,c}$ as a function of Hele-Shaw number H_S for different values of Lewis number L_e and modified diffusivity ratio N_A are illustrated in Figs. 6 and **7**, respectively.

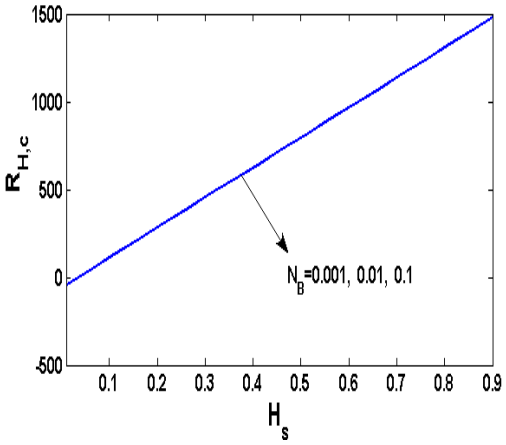

Fig. 4. Effect of the Hele-Shaw number H_s on the critical Hele-Shaw Rayleigh number $R_{H,c}$ for different values of modified particle density increment N_B with $R_{nH} = 1,\ N_A = 2,\ L_e = 50.$

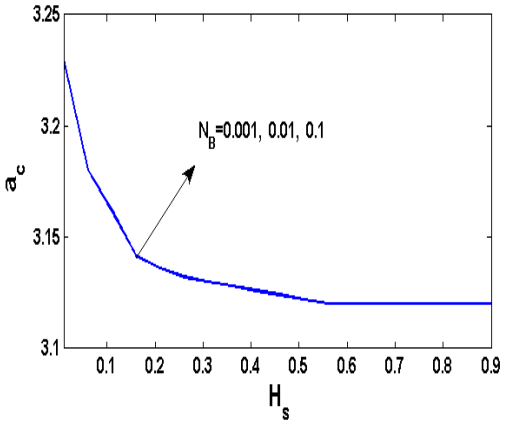

Fig. 5. Effect of the Hele-Shaw number H_s on the critical wave number a_c for different values of modified particle density increment N_B with $R_{nH} = 1,\ N_A = 2,\ L_e = 50.$

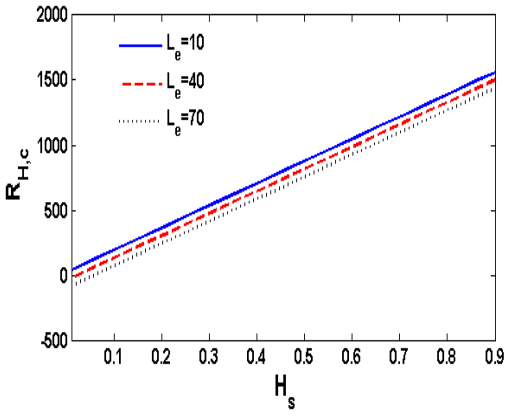

Fig. 6. Effect of the Hele-Shaw number H_s on the critical Hele-Shaw Rayleigh number $R_{H,c}$ for different values of Lewis number L_e with $R_{nH} = 1,\ N_A = 2,\ \mathrm{N_B} = 0.01.$

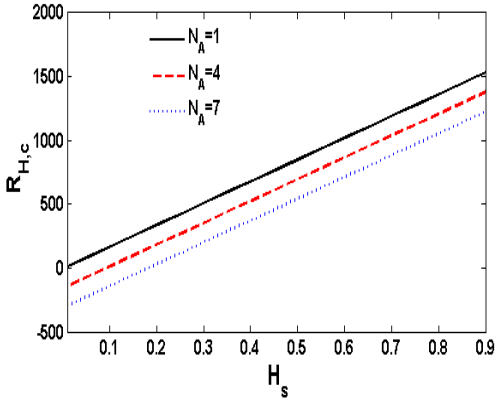

Fig. 7. Effect of the Hele-Shaw number H_s on the critical Hele-Shaw Rayleigh number $R_{H,c}$ for different values of modified diffusivity ratio N_A with $R_{nH} = 1$, $N_B = 0.01$, $L_e = 50$.

We found that with an increase in the values of the Lewis number L_e and the modified diffusivity ratio N_A, the critical Hele-Shaw Rayleigh number $R_{H,c}$ decreases, indicating that both accelerate the onset of convection in a nanofluid layer. It may be quality to the fact that the thermophoresis diffusivity is more supportable to the disturbance in nanofluids, while both thermophoresis and Brownian motion are driving forces in favour of the motion of nanoparticles.

The corresponding critical wave number a_c is plotted in Fig. 8 and shows that the critical wave number a_c does not depend on both the Lewis number L_e and the modified diffusivity ratio N_A. The effect of the Hele-Shaw number H_S is same as obtained in Figs. 2 and 3.

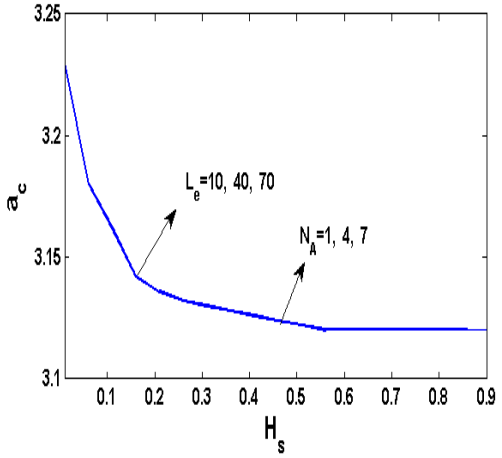

Fig. 8. Effect of the Hele-Shaw number H_s on the critical wave number a_c for different values of Lewis number L_e and modified diffusivity ratio N_A with $R_{nH} = 1$, $N_A = 2$, $N_B = 0.01$, $L_e = 50$.

To see the similarities as well as differences between the zero flux and the constant nanoparticle boundary conditions (Nield and Kuznetsov 2009) on the stability characteristics of the system, the critical Rayleigh number for different values of Hele-Shaw number H_S for these two boundary conditions are compared in Tables 2-4.

Table 2 Comparative results of $R_{H,c}$ and a_c for different values of H_s and R_{nH} with $N_A = 2$, $N_B = 0.01$, $L_e = 50$ for the (i) zero flux and (ii) the constant nanoparticle boundary conditions (Nield and Kuznetsov 2009)

H_s	a_c	R_{nH}	(i) R_c	(ii) R_c
0.01	3.23	0.5	9.40	34.40
	3.23	1	-41.60	8.40
	3.23	2	-143.60	-43.60
	3.23	3	-245.60	-95.60
0.1	3.15	0.5	164.06	189.06
	3.15	1	113.06	163.06
	3.15	2	11.06	111.06
	3.15	3	-90.94	59.06
1	3.12	0.5	1701.21	1726.21
	3.12	1	1650.21	1700.21
	3.12	2	1548.21	1648.21
	3.12	3	1446.21	1596.21

Table 3 Comparative results of the $R_{H,c}$ and a_c for H_s and L_e with $R_{nH} = 1$, $N_A = 2$, $N_B = 0.01$ for the (i) zero flux and (ii) the constant nanoparticle boundary conditions (Nield and Kuznetsov 2009)

H_s	a_c	L_e	(i) R_c	(ii) R_c
0.01	3.23	10	38.40	48.40
	3.23	30	-1.60	28.40
	3.23	50	-41.60	8.40
	3.23	70	-81.60	-11.60
0.1	3.15	10	193.06	203.06
	3.15	30	153.06	183.06
	3.15	50	113.06	163.06
	3.15	70	73.06	143.06
1	3.12	10	1730.21	1740.21
	3.12	30	1690.21	1720.21
	3.12	50	1650.21	1700.21
	3.12	70	1610.21	1680.21

From Tables 2-4, we obtained that the zero flux nanoparticle boundary condition has more destabilizing effect than the constant nanoparticle boundary conditions.

7. CONCLUSIONS

The onset of nanofluid convection in a vertically orientated Hele-Shaw cell was investigated numerically using linear stability theory. A more physical boundary condition where the nanoparticle fraction alters itself together with the consequence of Brownian and thermophoresis motions on the boundaries was taken. A comparison was also made between the existing boundary conditions for nanoparticle. The critical Hele-Shaw Rayleigh

number $R_{H,c}$ and the corresponding wave number a_c were obtained as a function of the Hele-Shaw number H_S for different values of the nanoparticle concentration Hele-Shaw Rayleigh number R_{nH}, the modified particle density increment N_B, the Lewis number L_e and the modified diffusivity ratio N_A. It was found that the nanoparticle concentration Hele-Shaw Rayleigh number, the Lewis number and the modified diffusivity ratio accelerate the onset of convection, while the Hele-Shaw number delays the onset of convection. The size of the convection cells depends only on the Hele-Shaw number H_S and increases with increasing H_S.

Table 4 Comparative results of the $R_{H,c}$ and the a_c for different values of H_s and N_A with $R_{nH}=1,\ \mathrm{N_B}=0.01,\ L_e=50$ for the (i) zero flux and (ii) the constant nanoparticle boundary conditions (Nield and Kuznetsov 2009)

H_s	a_c	N_A	(i) R_c	(ii) R_c
0.01	3.23	1	9.40	9.40
	3.23	3	-92.60	7.40
	3.23	5	-194.60	5.40
	3.23	7	-296.59	3.40
0.1	3.15	1	164.06	164.06
	3.15	3	62.04	162.06
	3.15	5	-39.94	160.06
	3.15	7	-141.94	158.06
1	3.12	1	1701.21	1701.21
	3.12	3	1599.21	1699.21
	3.12	5	1497.21	1697.21
	3.12	7	1395.21	1695.21

ACKNOWLEDGMENT

This work was supported by the Yonsei University Research Fund of 2014.

REFERENCES

Agarwal, S. (2014). Natural convection in a nanofluid-saturated rotating porous layer: A more realistic approach. *Transp. Porous Media* 104, 581-592.

Aybar, H., M. Sharifpur, M. R. Azizian, M. Mehrabi and J. P. Meyer (2014). A review of thermal conductivity models for nanofluids. *Heat Transfer Engineering* .

Bhadauria, B. S. and S. Agarwal (2011a). Natural convection in a nanofluid saturated rotating porous layer: a nonlinear study. *Transp Porous Media* 87, 585–602.

Bhadauria, B. S. and S. Agarwal (2011b). Convective transport in a nanofluid saturated porous layer with thermal non equilibrium model. *Transp. Porous Media* 88, 107–131.

Bhadauria, B. S., S. Agarwal and A. Kumar (2011). Non-linear two-dimensional convection in a nanofluid saturated porous medium. *Transp. Porous Media* 90, 605–625.

Bhadauria, B. S., P. K. Bhatia and L. Debnath (2005). Convection in Hele–Shaw cell with parametric excitation. *Int. J. Non-Linear Mech.* 40, 475-484.

Buongiorno, J. (2006). Convective transport in nanofluids. *Journal of Heat Transfer* 128, 240-250.

Chand, R. and G. C. Rana (2012). On the onset of thermal convection in rotating nanofluid layer saturating a Darcy-Brinkman porous medium. *Int. J. of Heat and Mass Transfer* 55, 5417-5424.

Chand, R. and G. C. Rana (2012). Thermal Instability of Rivlin–Ericksen elastico-viscous nanofluid saturated by a porous medium. *J. Fluids Eng.* 134, 121203.

Chand, R., G. C. Rana and A. K. Hussein (2015). On the onset of thermal instability in a low Prandtl number nanofluid layer in a porous medium. *Journal of Applied Fluid Mechanics* 8, 265-272.

Das, S. K., S. U. S. Choi and H. E. Patel (2006). Heat Transfer in Nanofluids-A Review. *Heat Transfer Engineering* 27, 3–19.

Elder, J. W. (1967). Steady free convection in a porous medium heated From below. *J. Fluid Mech.* 72, 29-48.

Guo, J. and P. N. Kaloni (1995). Double diffusive convection in porous medium, nonlinear study and Brinkman effect. *Stud. Appl. Math* 94, 341-358.

Hartline, B. K. and C. R. B. Lister (1977). Thermal convection in Hele–Shaw cell. *J. Fluid Mech.* 79, 379-389.

Hayat, T., M. Hussain, A. Alsaedi and S. Shehzad (2015). Flow of power-law nanofluid over a stretching surface with Newtonian heating. *Journal of Applied Fluid Mechanics* 8, 273-280.

Hele–Shaw, H. S. J. (1898). *Trans. Inst. Naval Archit* 40, 21.

Kuznetsov, A. V. (2011). Non-oscillatory and oscillatory nanofluid bio-thermal convection in a horizontal layer of finite depth. *European Journal of Mechanics-B/Fluids* 30, 156-165.

Kuznetsov, A. V. and D. A. Nield (2010). Thermal instability in a porous medium saturated by a nanofluid: Brinkman model. *Transp Porous Media* 81, 409–422.

Kuznetsov, A. V. and D. A. Nield (2010b). The onset of double-diffusive nanofluid convection in a layer of a saturated porous medium. *Transp. Porous Media* 85, 941–951.

Kuznetsov, A. V. and D. A. Nield (2010). Effect of

local thermal non-equilibrium on the onset of convection in porous medium layer saturated by a Nanofluid. *Transp Porous Media* 83, 425−436.

Kvernvold, O. (1979). On the stability of non linear convection in Hele–Shaw cell. *Int. J. Heat Mass Trans.* 22, 395-400.

Malvandi, A., F. Hedayati and D. D. Ganji (2015). Boundary layer slip flow and heat transfer of nanofluid induced by a permeable stretching sheet with convective boundary condition. *Journal of Applied Fluid Mechanics* 8, 151-158.

Manna, I. (2009). Synthesis, characterization and application of nanofluid: An overview. *Journal of the Indian Institute of Science* 89, 21-33.

Nield, D. A. and A. V. Kuznetsov (2009). Thermal instability in a porous medium layer saturated by a nanofluid. *Int. J Heat Mass Transf.* 52, 5796–5801.

Nield, D. A. and A. V. Kuznetsov (2011). The onset of double-diffusive convection in a nanofluid layer. *Int. J Heat Fluid Flow* 32, 771–776.

Nield, D. A. and A. V. Kuznetsov (2011). The effect of vertical through flow on thermal instability in a porous medium layer saturated by nanofluid. *Transp. Porous Media* 87, 765–775.

Nield, D. A. and A. V. Kuznetsov (2014). Thermal instability in a porous medium layer saturated by a nanofluid: A revised model. *Int. J. Heat Mass Transf.* 68, 211–214.

Rana, G. C., R. C. Thakur and S. K. Kango (2014). On the onset of double-diffusive convection in a layer of nanofluid under rotation saturating a porous medium. *J Porous Med.* 17, 657-667.

Tzou, D. Y. (2008). Thermal instability of nanofluids in natural convection. *International Journal of Heat and Mass Transfer* 51, 2967–2979.

Umavathi, J. C. and M. B. Mohite (2014). The onset of convection in a nanofluid saturated porous layer using Darcy model with cross diffusion. *Meccanica* 49, 1159-1175.

Wong, K. V. and T. Kurma (2008). Transport properties of alumina nanofluids. *Nanotechnology* 19, 345702.

Wooding, R. A. (1961). Instability of a viscous liquid of variable density in a vertical Hele-Shaw cell. *J. Fluid Mech.* 7, 501-515.

Xuan, Y. and Q. Li (2000). Heat Transfer Enhancement of Nano-Fluids. *International Journal of Heat and Fluid Flow* 21, 58–64.

Yadav, D., G.S. Agrawal, and R. Bhargava (2011). Thermal instability of rotating nanofluid layer. *Int. J Eng Sci.* vol. 49, pp. 1171–1184.

Yadav, D., R. Bhargava and G. S. Agrawal (2012a). Boundary and internal heat source effects on the onset of Darcy–Brinkman convection in a porous layer saturated by nanofluid. *Int. J Therm. Sci.* 60, 244–254.

Yadav, D., G. S. Agrawal and R. Bhargava (2012). The onset of convection in a binary nanofluid saturated porous layer. *Int. J. Theor. Appl. Multiscale Mech.* 2, 198–224.

Yadav, D., R. Bhargava and G. S. Agrawal (2013). Numerical solution of a thermal instability problem in a rotating nanofluid layer. *Int. J Heat Mass Transf.* 63, 313–322.

Yadav, D., R. Bhargava and G. S. Agrawal (2013). Thermal instability in a nanofluid layer with vertical magnetic field. *J. Eng. Math.* 80, 147-164.

Yadav, D., G. S. Agrawal and R. Bhargava (2013). The Onset of double-diffusive nanofluid convection in a layer of a saturated porous medium with thermal conductivity and viscosity variation. *Journal of Porous Media* 16, 105-121.

Yadav, D., R. Bhargava, G. S. Agrawal, N. Yadav, J. Lee and M. C. Kim (2014). Thermal instability in a rotating porous layer saturated by a non-Newtonian nanofluid with thermal conductivity and viscosity variation. *Microfluidics Nanofluidics 16, 425–440*.

Yadav, D. and M. C. Kim (2014). The effect of rotation on the onset of transient Soret-driven buoyancy convection in a porous layer saturated by a nanofluid. *Microfluidics and Nanofluidics 17, 1085-1093.*

Yadav, D. (2014). *Hydrodynamic and Hydromagnetic Instability in Nanofluids*. Lambert Academic Publishing, Germany.

Yu, W. and H. Xie (2012). A Review on Nanofluids: Preparation, Stability Mechanisms, and Applications. *Journal of Nanomaterials 1-17.*